

# Piperlongumine reduces ovalbumin-induced asthma and airway inflammation by regulating nuclear factor- $\kappa$ B activation

CHUN LU<sup>1,2\*</sup>, BING ZHANG<sup>2\*</sup>, TINGTING XU<sup>1</sup>, WENXIN ZHANG<sup>3</sup>, BIN BAI<sup>3</sup>, ZHONGXIANG XIAO<sup>2</sup>, LIQIN WU<sup>1</sup>, GUANG LIANG<sup>3</sup>, YALI ZHANG<sup>2,3</sup> and YUANRONG DAI<sup>1</sup>

<sup>1</sup>The Second Affiliated Hospital and Yuying Children's Hospital of Wenzhou Medical University, Wenzhou, Zhejiang 325000;

<sup>2</sup>Affiliated Yueqing Hospital, Wenzhou Medical University, Wenzhou, Zhejiang 325600; <sup>3</sup>Chemical Biology Research Center, School of Pharmaceutical Sciences, Wenzhou Medical University, Wenzhou, Zhejiang 325035, P.R. China

Received April 10, 2019; Accepted July 24, 2019

DOI: 10.3892/ijmm.2019.4322

**Abstract.** Asthma is a common chronic airway inflammatory disease, characterized by airway inflammation and remodeling. Piperlongumine (PL) has a number of physiological and pharmacological properties. However, the anti-asthmatic effect of PL has not been reported to date. In the present study, ovalbumin (OVA) was used to sensitize and challenge mice to induce asthma. The results revealed that PL pretreatment reduced OVA-induced airway inflammatory cell infiltration, reduced Th2 cytokine expression, both in the bronchoalveolar lavage fluid and in lung tissues, reduced the serum IgE level, pro-inflammatory cytokine [tumor necrosis factor (TNF)- $\alpha$  and interleukin (IL)-6] and intercellular adhesion molecule expression, as well as nuclear factor (NF)- $\kappa$ B activation. In addition, PL also mitigated OVA-induced goblet cell metaplasia, inhibited mucus protein secretion, mitigated airway

fibrosis and downregulated fibrosis marker expression. It was also demonstrated that PL inhibited TNF- $\alpha$  induced inflammatory cytokine expression and NF- $\kappa$ B activation *in vitro*. Taken together, the findings of the present study indicated that PL can reduce OVA-induced airway inflammation and remodeling in asthmatic mice, and that these effects may be mediated by inhibiting NF- $\kappa$ B signaling.

## Introduction

Asthma is a common chronic respiratory disease that affects >334 million people worldwide, and is characterized by inflammation, airway hyperresponsiveness (AHR), mucus hypersecretion and airway remodeling (1,2). The clinical symptoms of asthma are non-specific, and include wheezing, shortness of breath, chest tightness and/or cough (2). The pathogenesis of asthma is complex and has not yet been fully elucidated. In recent years, imbalance of Th1/Th2 cells resulting from overactivation of Th2 cells has been recognized as the immunological basis of asthma (3,4). Following stimulation by exogenous allergens, the body activates Th0 cells to differentiate into CD4<sup>+</sup> Th2 cells, which secrete interleukin (IL)-4, IL-5, IL-13 and other cytokines (4). These cytokines promote B-cell secretion of immunoglobulin (Ig)E, hyperplasia of eosinophils, bronchial epithelial cells, mast cells and goblet cells, hypersecretion of mucus and AHR, leading to the development of asthma (5,6).

There is currently no definitive clinical cure for asthma. As this is a chronic inflammatory airway disease, relieving airway inflammation is key to managing asthma (7). Airway inflammation persists throughout the course of the disease and lays the basis for AHR, which is a common characteristic of asthma (5). In the clinical setting, the most commonly used drugs include inhaled corticosteroids (ICS) combined with long-acting  $\beta$ 2 agonists (LABA), theophylline, M cholinergic receptor blockers and leukotriene receptor antagonists (1,8). The most commonly used pharmacological approach to asthma is daily administration of ICS together with LABA (8). However, there may be inconsistencies between different patients in terms of symptom control and worsening of asthma during treatment. Continuing to increase the ICS dose in patients who continue to deteriorate or those with

*Correspondence to:* Professor Yuanrong Dai, The Second Affiliated Hospital and Yuying Children's Hospital of Wenzhou Medical University, 109 Xueyuanxi Road, Wenzhou, Zhejiang 325000, P.R. China  
E-mail: daiyr@126.com

Dr Yali Zhang, Chemical Biology Research Center, School of Pharmaceutical Sciences, Wenzhou Medical University, Central North Road, Chashan University Town, Wenzhou, Zhejiang 325035, P.R. China  
E-mail: ya-li000@163.com

\*Contributed equally

**Abbreviations:** AHR, airway hyperresponsiveness; BALF, bronchoalveolar lavage fluid; cDNA, complementary DNA; H&E, hematoxylin and eosin; ICS, inhaled corticosteroids; IgE, immunoglobulin E; LABA, long-acting  $\beta$ 2 agonists; MTT, methyl thiazolyl tetrazolium; OVA, ovalbumin; PAS, periodic acid-Schiff; PBS, phosphate-buffered saline; PL, piperlongumine; RT-qPCR, reverse transcription-quantitative polymerase chain reaction; SEM, standard error of the mean

**Key words:** piperlongumine, ovalbumin, asthma, airway inflammation, airway remodeling

persistent symptoms may be associated with side effects such as spread of infection, increased incidence of gastric ulcers, gastrointestinal bleeding, hypertension, increased blood sugar levels, sodium retention and low serum potassium levels, among others (9,10). In addition, although the introduction of monoclonal antibodies that target the IL-5 pathway confers a significant advantage by reducing eosinophilic inflammation with subsequent symptom improvement in asthmatic patients, a proportion of asthmatic patients have been found to be IL-5-independent (11-13). Thus, there is an urgent need for effective and safe drugs for the treatment of asthma.

Piperlongumine (PL; Fig. 1A), an amide compound isolated from the root of *Piper longum* Linn, has several physiological and pharmacological properties, including analgesic, sedative, anti-inflammatory, anxiolytic, antidepressant and antitumor properties (14). Its antitumor activity has been extensively investigated in several types of cancer, and was found to exert selective cytotoxic effects against tumor cells (15,16). In recent years, researchers have reported that PL and its analogs act as anti-inflammatory agents, as they inhibit lipopolysaccharide-induced inflammation, collagen-induced arthritis and neuroinflammation (17-19). However, there is currently no literature on the anti-asthmatic effects of PL. Therefore, the aim of the present study was to investigate whether PL treatment can reduce ovalbumin (OVA)-induced asthma in mice and elucidate the potential underlying mechanism.

## Materials and methods

**Animals.** Male C57BL/6 mice, weighing 18-22 g, were obtained from the Animal Center of Wenzhou Medical University. All animals were housed at constant room temperature with a 12:12-h light: Dark cycle, and fed a standard rodent diet and water. All animals were allowed to acclimatize for at least 3 days before the experiments. Animal care and experimental protocols were approved by the Committee on Animal Care of Wenzhou Medical University (approval document no. wyd2017-0027).

**OVA-induced asthma.** A total of 35 mice were randomly divided into five groups (n=7 per group) as follows: Mice sensitized with phosphate-buffered saline (PBS) and administered equal volumes of 0.5% carboxymethylcellulose sodium (CMCNa; CON group) or 10 mg/kg PL (PL10 group) intragastrically; mice sensitized with OVA and administered equal volume of 0.5% CMCNa (OVA group); mice sensitized with OVA and treated with 5 or 10 mg/kg PL (PL5 + OVA or PL10 + OVA groups, respectively). The flowchart of the experimental design is shown in Fig. 1B. Mice were sensitized on days 0 and 14 with an intraperitoneal (i.p.) injection of 20  $\mu$ g OVA (Sigma-Aldrich; Merck KGaA) emulsified with 2 mg aluminum hydroxide (Sigma-Aldrich; Merck KGaA) in 200  $\mu$ l PBS (pH 7.4). On days 25-31, the mice were subjected to an airway challenge with 1% OVA or PBS for 30 min delivered with a PARI TurboBOY N medical compressed air nebulizer (PARI GmbH). At 30 min prior to the OVA inhalation challenge, the mice were intragastrically administered PL dissolved in 0.5% CMCNa. One day after the last challenge, the mice were anesthetized by i.p. injection of sodium pentobarbital (60 mg/kg) and blood was collected for further

analysis. The mice were then sacrificed by i.p. injection of 200 mg/kg sodium pentobarbital, followed by collection of bronchoalveolar lavage fluid (BALF) and lung tissue.

**Serum and BALF collection and analysis.** Blood was collected from the orbital vascular plexus and centrifuged at 15,777 x g for 10 min. The serum was collected and stored at -80°C. To obtain BALF, PBS (200  $\mu$ l) was infused into the left lung four times (total volume, 800  $\mu$ l). The collected BALF was centrifuged at 110 x g for 10 min at 4°C. The supernatant was collected and stored at -80°C and the precipitate was resuspended in 40  $\mu$ l PBS. The total number of cells in BALF was determined with a cell counting instrument. The number of eosinophils in BALF was examined by Wright-Giemsa staining.

**Histopathological study.** The middle lobe of the right lung was collected and fixed in 4% paraformaldehyde, then embedded in paraffin and cut into 5- $\mu$ m sections. The areas of inflammation, severe fibrosis and mucus secretion were analyzed by hematoxylin and eosin (H&E), Sirius Red and periodic acid-Schiff (PAS) staining, respectively. The sections were stained using standard protocols for light microscopy examination. A pathologist blindly determined the histopathological score according to the following two categories: Peribronchial inflammation and perivascular inflammation. A value of 0-3 per criterion was assigned to each tissue section as follows: 0, no inflammatory cells; 1, occasional cuffing with inflammatory cells; 2, most bronchi or vessels surrounded by a thin layer (1-5) of inflammatory cells; 3, most bronchi or vessels surrounded by a thick layer (>5 cells). Subepithelial fibrosis was estimated by dividing the area of Sirius Red staining by the length of the bronchiolar basement membrane. PAS-staining was identified using Image J software (National Institutes of Health), and the pixel intensities of each color channel (red, blue and green) were averaged. The mucus index was determined using the following equation: Mucus index = [(area of PAS staining) x (mean intensity of PAS staining)]/[total area of airway epithelium (including PAS staining)] (20). The final indices were the results of a mean of 5 images per lung, encompassing large and small bronchial airways.

**Measurement of AHR.** AHR was determined by measuring the changes in airway resistance (Rn) after the mice were subsequently exposed to increasing concentrations of methacholine (Mch; 3.125-50 mg/ml; Sigma-Aldrich; Merck KGaA) in PBS using the flexiVent system (SCIREQ). After the mice were anesthetized with 1% pentobarbital sodium (50 mg/kg), tracheostomy was performed and the tracheostomized mice were mechanically ventilated at 200 breaths/min with a tidal volume of 10 ml/kg under appropriate anesthesia. Mch aerosol was challenged for 10 sec, after which time airway resistance was continuously monitored and recorded.

**Immunohistochemistry (IHC).** Lung sections (5  $\mu$ m) were prepared, deparaffinized in xylene, and rehydrated using an ethanol gradient. A pressure cooker was used for antigen retrieval (10 mM sodium citrate buffer, pH 6.0). After using 3% hydrogen peroxide to remove catalase, all sections were blocked in 1% bovine serum albumin (BSA) for 30 min, then

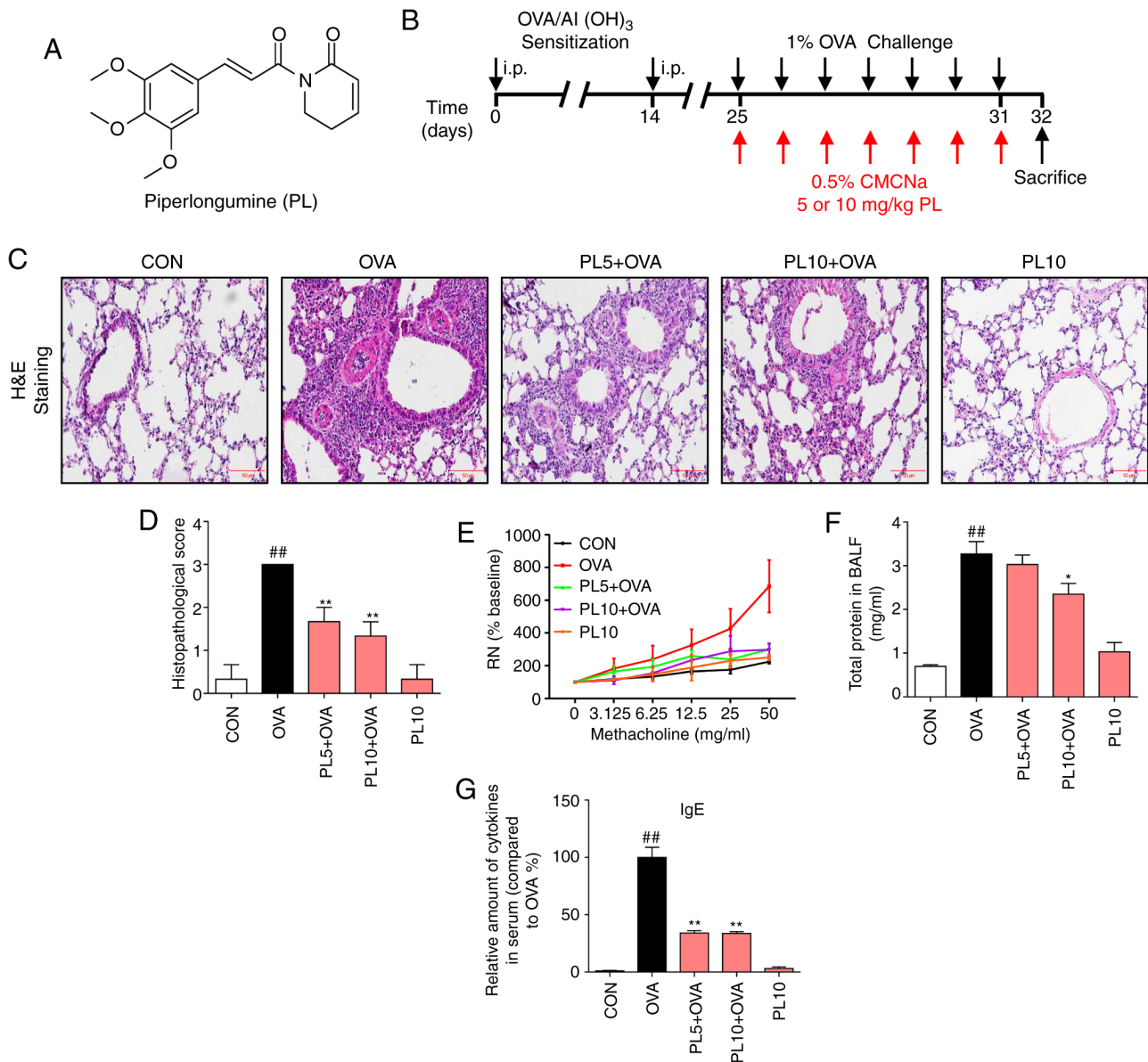


Figure 1. Effects of PL on OVA-induced asthma. (A) Chemical structure of PL. (B) Schematic diagram describing the workflow of the experiment. (C) H&E staining was performed to evaluate OVA-induced inflammation and lung injury in asthma (magnification, x200). (D) Scoring of inflammation was conducted through pathological evaluation of the inflammatory cell infiltrate in lung sections. (E) AHR was assessed as the mean response to increased doses of Mch by mechanical ventilation in mice. (F) Total protein concentration in BALF. (G) The serum IgE levels were determined by ELISA. Data are presented as the mean  $\pm$  standard error of the mean. <sup>##</sup>P<0.01 vs. CON group; <sup>\*</sup>P<0.05, <sup>\*\*</sup>P<0.01 vs. OVA group. PL, piperlongumine; OVA, ovalbumin; H&E, hematoxylin and eosin; AHR, airway hyperresponsiveness; Mch, methacholine; BALF, bronchoalveolar lavage fluid; CMCNa, carboxymethylcellulose sodium.

incubated with TNF- $\alpha$  (mouse monoclonal, dilution: 1:200, cat. no. ab1793, Abcam) or  $\alpha$ -smooth muscle actin (SMA; mouse monoclonal, dilution: 1:200, cat. no. ab7817, Abcam) antibody overnight at 4°C, followed by incubation with secondary antibody for 60 min at 37°C. After the sections were incubated with 3,3-diaminobenzidine tetrahydrochloride for color development, they were counterstained with hematoxylin and visualized under a light microscope. The percentage expression of  $\alpha$ -SMA or TNF- $\alpha$  in 10 fields of view was analyzed by Image J software (National Institutes of Health).

**Cell culture and treatment.** The human bronchial epithelial cell line Beas-2B was obtained from the Cell Bank of the Chinese Academy of Sciences. The cells were cultured in RPMI-1640 (Gibco; Thermo Fisher Scientific, Inc.) supplemented with

20% fetal bovine serum (HyClone; GE Healthcare Life Sciences) and 1% penicillin/streptomycin in a humidified atmosphere at 37°C with 5% CO<sub>2</sub>. Beas-2B cells were treated with DMSO or PL (5 or 10  $\mu$ M) for 30 min, and then treated with or without 5 ng/ml TNF- $\alpha$  for an additional 24 h to collect medium, 12 h to collect mRNA, and 30 min to collect protein.

**Western blot assay.** Lung tissue homogenate (100  $\mu$ g) and cell protein (30  $\mu$ g) samples were subjected to 10% sodium dodecyl sulfate polyacrylamide gel electrophoresis and transferred to PVDF membranes (Bio-Rad Laboratories, Inc.). After blocking with 5% milk, the membranes were probed with a specific primary antibody against I $\kappa$ B $\alpha$  (rabbit monoclonal, dilution 1:1,000, cat. no. 4812, Cell Signaling Technology Inc) and  $\beta$ -actin (mouse monoclonal, dilution: 1:1,000, cat.

Table I. The sequences of primer used for reverse transcription-quantitative polymerase chain reaction analysis.

Gene	Species	Forward primer (5'-3')	Reverse primer (5'-3')
$\beta$ -actin	Mouse	CCGTGAAAAGATGACCCAGA	TACGACCAGAGGCATACAG
ICAM-1	Mouse	GCCTTGGTAGAGGTGACTGAG	GACCGGAGCTGAAAAGTTGTA
IL-4	Mouse	CCATATCCACGGATGCGACA	CTGTGGTGTTCCTTCGTTGCTG
IL-5	Mouse	CAAGCAATGAGACGATGAGGC	AGCATTTCACAGTACCCCC
IL-6	Mouse	CCAAGAGGTGAGTGCTTCCC	CTGTTGTTTCAGACTCTCTCCCT
IL-13	Mouse	GTTCTCTCACTGGCTCTGGG	CAGGGGAGTCTGGTCTTGTG
MMP-9	Mouse	TCTTCTGGCGTGTGAGTTTCC	CGGTTGAAGCAAAGAAGGAGC
Muc5ac	Mouse	GTCCTGAGGGTATGGTGCTTG	CATGTGTTGGTGCAGTCAGTAG
Muc5b	Mouse	TGGCCTTGCTCATGGTGTG	TGTAAGGCGCTCATGCTAGG
TNF- $\alpha$	Mouse	TGATCCGCGACGTGGAA	ACCGCCTGGAGTTCTGGAA
$\beta$ -actin	Human	CCTGGCACCCAGCACAAAT	GCCGATCCACACGGAGTACT
ICAM-1	Human	GAACCAGAGCCAGGAGACAC	TCCCTTTTTGGGCCTGTTGT
IL-1 $\beta$	Human	ACGCTCCGGGACTCACAGCA	TGAGGCCCAAGGCCACAGGT
IL-6	Human	GCACTGGCAGAAAACAACCT	TCAAACCTCCAAAAGACCAGTGA
MCP-1	Human	TCACCTGCTGCTACTCATTACCA	TACAGCTTCTTTGGGACACCTGCT

ICAM, intracellular adhesion molecule; IL, interleukin; MMP, matrix metalloproteinase; TNF, tumor necrosis factor; MCP, monocyte chemoattractant protein.

no. ab8226, Abcam) overnight at 4°C. The membranes were then washed and incubated with corresponding secondary antibody (Yeasten). The blots were visualized using enhanced chemiluminescence reagents (Bio-Rad Laboratories Inc.). The density of the immunoreactivity bands was analyzed using Image J software (National Institutes of Health).

**Methyl thiazolyl tetrazolium (MTT) assay.** Beas-2B cells were seeded into 96-well plates at a density of 3,000 cells per well. PL was dissolved in DMSO and diluted with RPMI-1640. The cells were incubated with different concentrations of PL (1.25, 2.5, 5, 10, 20 and 40  $\mu$ M) for 24 h prior to the MTT assay. A fresh solution of MTT (5 mg/ml) prepared in PBS was added to each well. The plate was then incubated in a CO<sub>2</sub> incubator for 4 h, formazan crystals were dissolved with 150  $\mu$ l DMSO, and analyzed in a multi-well-plate reader at 490 nm.

**RNA isolation and reverse transcription-quantitative polymerase chain reaction (RT-qPCR) analysis.** Total RNA was prepared using TRIzol reagent (Invitrogen; Thermo Fisher Scientific, Inc.) and quantified by ultraviolet absorption at 260 and 280 nm. Complementary DNA (cDNA) was generated from 2  $\mu$ g total RNA using a cDNA synthesis kit (Invitrogen; Thermo Fisher Scientific, Inc.). Then cDNA gene expression was assayed by qPCR with SYBR-Green qPCR Super Mix-UDG kit on a Mastercycler<sup>®</sup> ep realplex detection system (Eppendorf). The relative mRNA levels were calculated with the 2<sup>- $\Delta\Delta$ C<sub>t</sub></sup> method (21) using  $\beta$ -actin as an internal control. The sequences of the sense and antisense primers are listed in Table I.

**Enzyme-linked immunosorbent assay (ELISA).** The levels of IL-4, IL-5 and IL-13 in BALF supernatants and lung homogenates and the IL-1 $\beta$  level in cell culture supernatants were

detected using ELISA kits (eBioScience) according to the manufacturer's instructions.

**Statistical analysis.** Data collected from the experiments were analyzed using Graphpad Prism 7.0 software (GraphPad Software, Inc.). Values are expressed as mean  $\pm$  standard error of the mean. One-way analysis of variance followed by Dunnett's post hoc test was employed to analyze the differences between sets of data. A P-value of <0.05 was considered to indicate statistically significant differences.

## Results

**PL alleviates OVA-induced lung injury and IgE production.** C57BL/6 mice were sensitized and challenged with OVA for 31 days to induce asthma (Fig. 1B). On the 32nd day, the mice were sacrificed, and lung tissues and BALF were collected 24 h after the last challenge with OVA. The histological sections revealed that the lung tissues from both the CON and PL10 groups had normal morphology, with thin-lined alveolar septa and well-organized alveolar spaces (Fig. 1C). Administration of OVA induced severe alveolar injury, with thickened intra-alveolar septa, collapsed alveolar spaces, edema and inflammatory cell infiltration. Treatment with PL significantly mitigated OVA-induced lung injury. The quantification of lung injury score is shown in Fig. 1D. Furthermore, AHR was established with Mch to determine whether PL exerts any effects on AHR. As shown in Fig. 1E, OVA sensitization and challenge led to an increased Rn value in response to increasing concentrations of Mch. However, the PL (5 and 10 mg/kg) groups exhibited significantly lower Rn values compared with the OVA-treated group. Moreover, the total BALF protein concentration was markedly increased in OVA-challenged mice, and treatment with PL dose-dependently lowered the protein levels,

suggesting that treatment with PL reduces pulmonary permeability (Fig. 1F). Furthermore, the total IgE levels in the serum were higher in OVA-sensitized mice compared with those in CON group mice (Fig. 1G). Treatment with PL effectively reduced the increased serum IgE levels induced by OVA.

**PL alleviates OVA-induced airway remodeling.** Airway remodeling is a common characteristic of asthma, which is reflected by basement membrane thickening, subepithelial fibrosis, airway smooth muscle proliferation, goblet cell metaplasia and increased mucus secretion. PAS staining was performed to evaluate goblet cell metaplasia in the airway epithelium. As shown in Fig. 2A, marked goblet cell metaplasia was observed in OVA-induced asthmatic lung tissue, which was significantly reduced by either dose of PL. The quantified results revealed that PL effectively mitigated goblet cell metaplasia in a dose-dependent manner (Fig. 2B). To further assess the goblet cell response in asthmatic mice, the levels of Muc5AC and Muc5B were measured by RT-qPCR (Fig. 2C and D). OVA sensitization and challenge increased the mRNA levels of Muc5AC and Muc5B, while in mice treated with PL this increase was reversed. The degree of subepithelial fibrosis was evaluated by Sirius Red staining (Fig. 2E) and  $\alpha$ -SMA IHC staining (Fig. 2G). As shown in Fig. 2E and G, OVA-sensitized mice exhibited high levels of subepithelial collagen and  $\alpha$ -SMA, respectively. However, PL treatment reduced the OVA-induced increase in collagen and  $\alpha$ -SMA levels in lung tissues. The quantified results also revealed that PL dose-dependently reduced the OVA-induced increase in collagen and  $\alpha$ -SMA levels (Fig. 2F and H). Matrix metalloproteinase (MMP)-9 participated in airway remodeling, which contributes to airway narrowing. OVA upregulated the MMP-9 mRNA levels in lung tissue, and this effect was inhibited by PL treatment (Fig. 2I). Therefore, airway remodeling was more pronounced in OVA mice compared with control group mice, and PL treatment significantly inhibited airway remodeling, including subepithelial fibrosis, airway smooth muscle proliferation, goblet cell metaplasia and increased mucus secretion.

**PL alleviates OVA-induced IL-4, IL-5 and IL-13 expression in the BALF and lung tissue at the protein and mRNA level.** In addition to airway remodeling, airway Th2 inflammation is a major characteristic of asthma. IL-4, IL-5 and IL-13 are well-recognized inflammatory factors secreted by Th2 effector cells. Thus, the protein and mRNA levels of IL-4, IL-5 and IL-13 were measured by ELISA and RT-qPCR assay, respectively. As shown in Fig. 3A-F, the protein levels of IL-4, IL-5 and IL-13 in the BALF and lung tissue were upregulated by OVA sensitization, and this effect was inhibited by PL treatment. In addition, the mRNA levels of IL-4 (Fig. 3G), IL-5 (Fig. 3H) and IL-13 (Fig. 3I) in lung tissue were upregulated in the OVA group and downregulated in the PL treatment group. The results of the present study demonstrated that PL significantly decreased the OVA-induced upregulation of IL-4, IL-5 and IL-13 at the protein and mRNA levels.

**PL alleviates OVA-induced inflammation by inhibiting the activation of the NF- $\kappa$ B pathway.** OVA sensitization is associated with large numbers of inflammatory cells in the BALF,

including eosinophils, while PL treatment reduced the total number of inflammatory cells (Fig. 4A) and eosinophils (Fig. 4B) in the BALF. TNF- $\alpha$  is a major pro-inflammatory cytokine that is considered to be crucial for the pathogenesis of asthma. OVA was found to increase the protein and mRNA levels of TNF- $\alpha$  in BALF and lung tissue, as detected by ELISA (Fig. 4C), IHC staining (Fig. 4D and E) and RT-qPCR assay (Fig. 4F), while these increases were significantly reduced by PL treatment. Another pro-inflammatory cytokine, IL-6 (Fig. 4G), and intracellular adhesion molecule (ICAM)-1 (Fig. 4H) were also found to be markedly increased in OVA-challenged mice compared with the CON group. However, treatment with PL inhibited the upregulation of IL-6 and ICAM-1. To elucidate the underlying mechanism through which PL reduces OVA-induced inflammatory response, NF- $\kappa$ B pathway activation was investigated. I $\kappa$ B $\alpha$  is an inhibitory protein of NF- $\kappa$ B, the degradation of which can activate the NF- $\kappa$ B signaling pathway. As shown in Fig. 4I, the protein level of I $\kappa$ B $\alpha$  was downregulated in the lung tissue of OVA group compared with CON group mice. However, PL treatment dose-dependently reversed the I $\kappa$ B $\alpha$  degradation. These results indicate that PL reduces OVA-induced inflammatory response by inhibiting the activation of the NF- $\kappa$ B pathway.

**PL alleviates TNF- $\alpha$  induced inflammation by inhibiting NF- $\kappa$ B activation in Beas-2B cells.** Our *in vivo* results verified that PL appears to relieve OVA-induced asthma and airway inflammation by inhibiting NF- $\kappa$ B activation. To further confirm the effects of PL on inflammatory response and the NF- $\kappa$ B pathway, TNF- $\alpha$  was used to induce inflammation in Beas-2B cells. First, the cytotoxicity of PL on Beas-2B cells was detected (Fig. 5A). Treatment with PL caused cell viability to decrease at concentrations of  $\geq 10 \mu\text{M}$ . Therefore, PL was used at 2.5 and 5  $\mu\text{M}$  for further experiments. TNF- $\alpha$  treatment significantly induced the protein (Fig. 5B) and mRNA (Fig. 5C) levels of IL-1 $\beta$ , IL-6 (Fig. 5D), the chemokine monocyte chemoattractant protein (MCP)-1 (Fig. 5E) and the adhesion molecule ICAM-1 (Fig. 5F) in Beas-2B cells, while pretreatment with PL dose-dependently inhibited this increase. In addition, TNF- $\alpha$  treatment downregulated the I $\kappa$ B $\alpha$  protein level, while pretreatment with PL reversed the degradation of I $\kappa$ B $\alpha$  (Fig. 5G and H).

## Discussion

The most significant finding of the present study is that PL treatment inhibited the development of airway inflammation, inflammatory cell infiltration and airway remodeling in mice with OVA-induced asthma. The effect of PL on OVA-induced airway inflammation was mostly mediated by inhibiting the activation of the NF- $\kappa$ B pathway.

Accumulating evidence suggests that asthma is a heterogeneous disorder regulated by distinct molecular mechanisms. Recent studies have indicated that the imbalance between the Th1 and Th2 subsets of Th cells, particularly the abnormal activation of Th2 cells, is closely associated with the pathogenesis of asthma (22,23). Patients with Th2-high asthma have prominent eosinophilia and high levels of Th2 cytokines, namely IL-4, IL-5 and IL-13 (24). IL-4 is key to the activation, classification and regulation of B lymphocyte function,

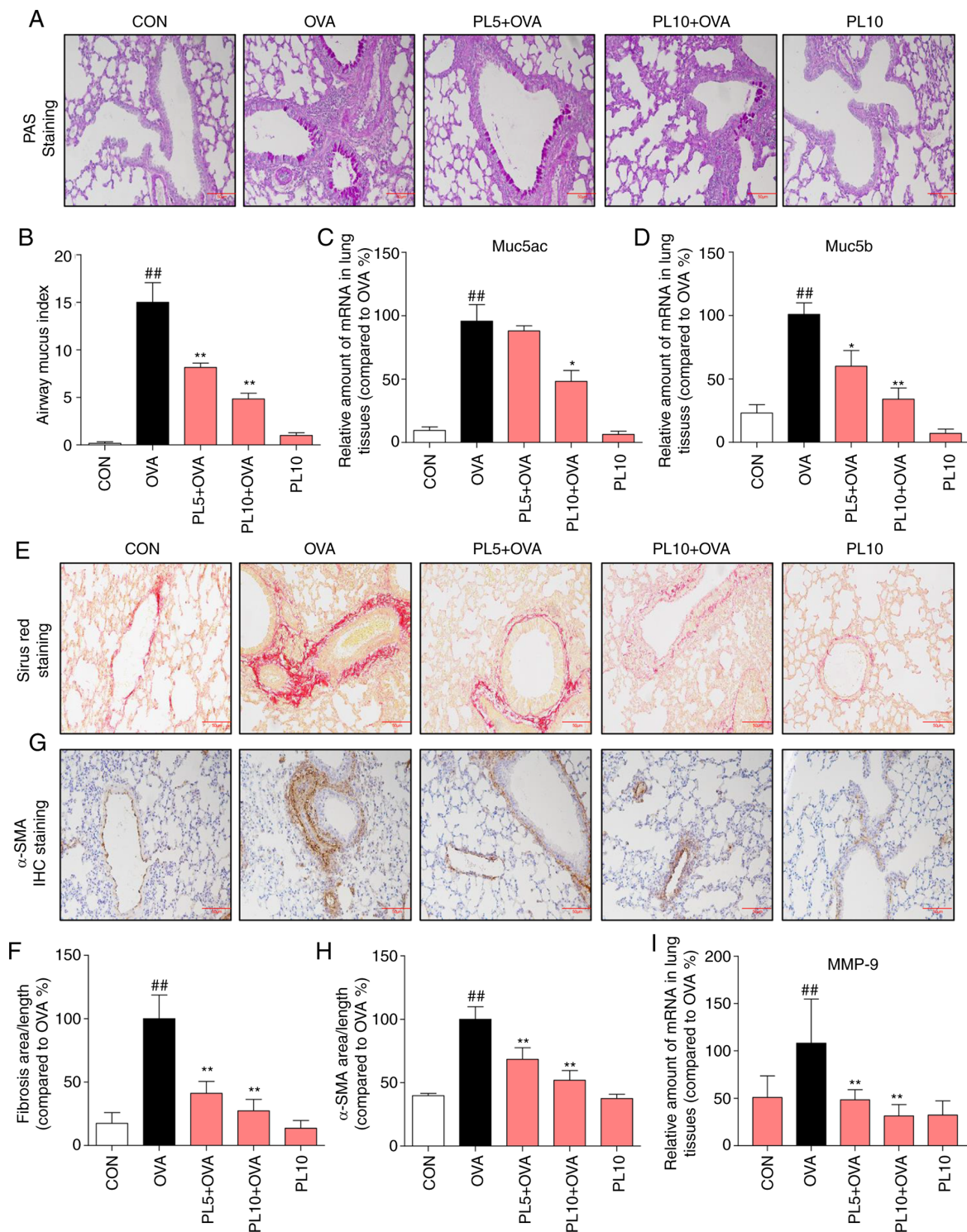


Figure 2. PL reduces OVA-induced airway remodeling. (A) PAS staining was performed to evaluate goblet cell metaplasia (magnification, x200). (B) Quantification of airway mucus. RT-qPCR assay was performed to detect the (C) Muc5ac and (D) Muc5b gene levels in lung tissues. (E) OVA-induced collagen deposition was detected by Sirius Red staining (magnification, x200). (F) Quantification of the area of fibrosis in lung tissue as detected by Sirius Red staining. (G) Representative immunostaining of peribronchial  $\alpha$ -SMA in lung tissue (magnification, x200). (H) Quantification of the percentage expression of  $\alpha$ -SMA protein in lung tissue. (I) Gene expression of MMP-9 was determined by RT-qPCR analysis. Data are presented as the mean  $\pm$  standard error of the mean. <sup>##</sup> $P < 0.01$  vs. CON group; <sup>\*</sup> $P < 0.05$ , <sup>\*\*</sup> $P < 0.01$  vs. OVA group. PL, piperlongumine; OVA, ovalbumin; PAS, Periodic acid-Schiff; RT-qPCR, reverse transcription-quantitative polymerase chain reaction; SMA, smooth muscle actin; MMP, matrix metalloproteinase.

and it contributes to the regulation of IgE in inflammation by enhancing the combination of IgE and related antibodies (25). IL-5 markedly affects the formation of eosinophils and promotes their growth, activation and differentiation, and it also enhances their migration to inflammatory sites (26). IL-13,

a pleiotropic cytokine, is 20-25% identical and has similar effector functions with IL-4 in the context of type II immune response (27). In the present study, asthmatic mice exhibited increased total inflammatory cell count and eosinophil infiltration in the BALF, increased IgE and Th2 cytokine expression

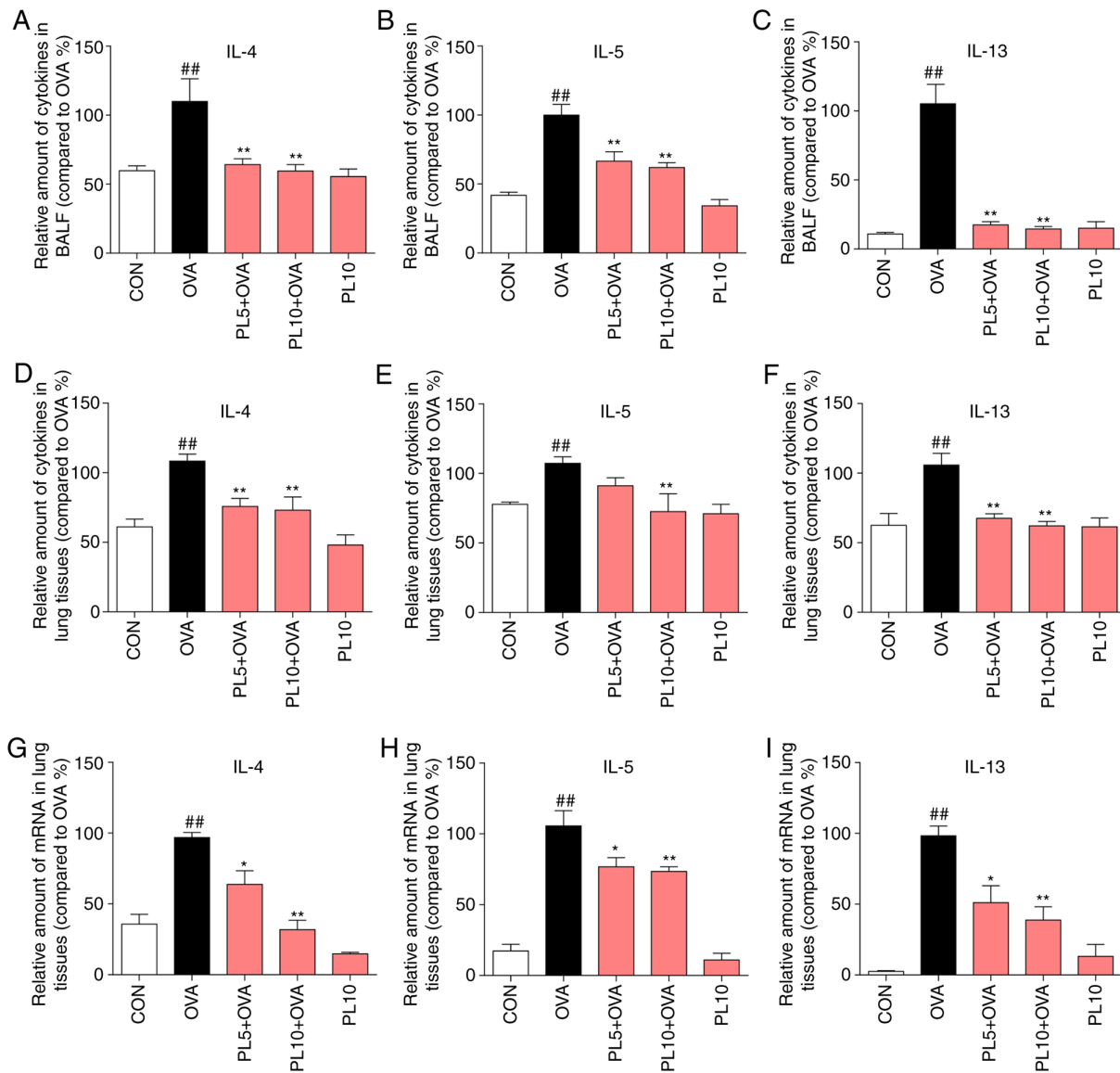


Figure 3. PL reduces OVA-induced IL-4, IL-5 and IL-13 expression in the BALF and lung tissue at the protein and mRNA levels. The levels of IL-4, IL-5 and IL-13 in (A-C) the BALF and (D-F) lung tissue were detected by ELISA. (G-I) The mRNA levels of (G) IL-4, (H) IL-5 and (I) IL-13 were determined by RT-qPCR analysis using  $\beta$ -actin mRNA as the internal control. Data are presented as the mean  $\pm$  standard error of the mean. ##P<0.01 vs. CON group; \*P<0.05, \*\*P<0.01 vs. OVA group. PL, piperlongumine; OVA, ovalbumin; IL, interleukin; BALF, bronchoalveolar lavage fluid; RT-qPCR, reverse transcription-quantitative polymerase chain reaction.

in the BALF and lung tissue, while pretreatment with PL mitigated inflammatory cell infiltration and downregulated cytokine expression. However, an inflammatory cell differential count in the BALF was not conducted, as the asthma model we used in this study was eosinophil-predominant.

Airway remodeling is a major characteristic of asthma, and has important functional implications (28). Although some aspects of airway remodeling may be explained as a consequence of Th2 inflammation, remodeling occurs by way of a non-inflammatory mechanism according to several publications (29,30). In the present acute asthma mouse model, collagen deposition was obviously induced by repeated OVA challenging (7 times). This result was consistent with the results of An *et al*, who reported that OVA can induce collagen deposition after challenging for 3 continuous days (30). However, there was no obvious difference in basement membrane thickening between the CON and OVA groups, or between the two

PL treatment groups (data not shown). A possible explanation for the airway remodeling occurring in an acute asthma model may be that airway inflammation and remodeling occur in parallel and not sequentially.

TNF- $\alpha$  is a pleiotropic inflammatory cytokine binding to the type 1 TNF receptor (31). Two clinical trials demonstrated that the TNF- $\alpha$  expression was upregulated in patients with refractory asthma and in children with mild-to-severe asthma when compared with normal controls (32,33). Healthy individuals who were subjected to recombinant TNF- $\alpha$  inhalation may display bronchial hyperresponsiveness (34). TNF- $\alpha$  can also upregulate the expression of adhesion molecules, such as vascular cell adhesion molecule-1 and ICAM-1, thereby inducing inflammatory cell influx into the lung and airways. In the present study, asthmatic mice exhibited increased levels of TNF- $\alpha$  in the BALF and lung tissues, as determined by ELISA, TNF- $\alpha$  IHC staining and RT-qPCR assay. Administration

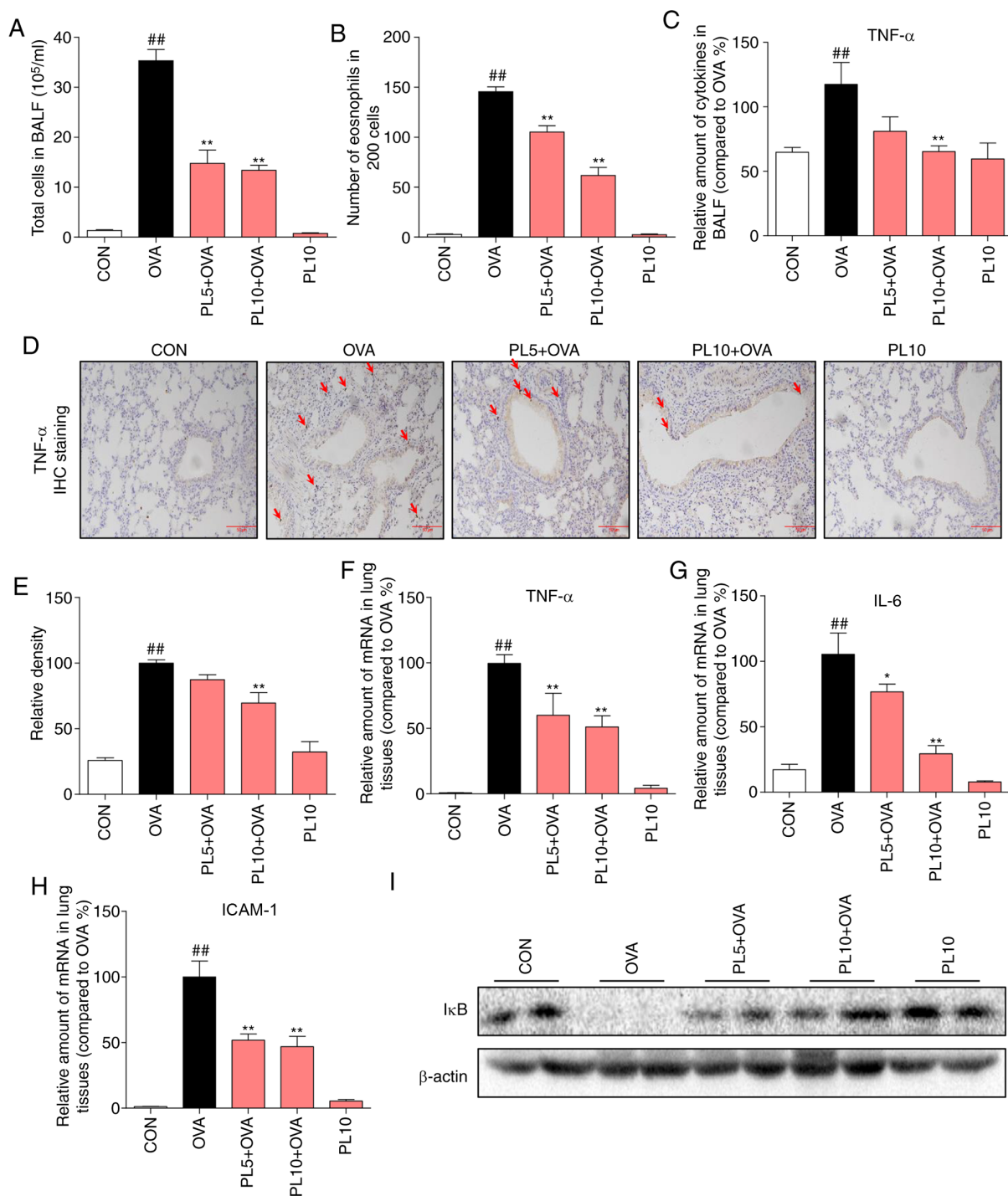


Figure 4. PL reduces OVA-induced inflammation by inhibiting activation of the NF- $\kappa$ B pathway. Number of (A) total cells and (B) eosinophils in the BALF. (C) The level of TNF- $\alpha$  in the BALF was determined by ELISA. (D) Representative TNF- $\alpha$  immunostaining (arrows; magnification, x200) of lung tissue. (E) Quantification of the percentage expression of the TNF- $\alpha$  protein in lung tissue. (F-H) The mRNA levels of TNF- $\alpha$ , IL-6 and ICAM-1 were determined by RT-qPCR analysis using  $\beta$ -actin mRNA as the internal control. (I) Protein levels of I $\kappa$ B and  $\beta$ -actin was detected by western blotting. Data are presented as the mean  $\pm$  standard error of the mean. <sup>##</sup>P<0.01 vs. CON group; <sup>\*</sup>P<0.05, <sup>\*\*</sup>P<0.01 vs. OVA group. PL, piperlongumine; OVA, ovalbumin; NF- $\kappa$ B, nuclear factor- $\kappa$ B; BALF, bronchoalveolar lavage fluid; TNF, tumor necrosis factor; IL, interleukin; ICAM, intracellular adhesion molecule; RT-qPCR, reverse transcription-quantitative polymerase chain reaction.

of PL at 10 mg/kg significantly reduced TNF- $\alpha$  expression levels. As TNF- $\alpha$  is crucial for the development of asthma and airway inflammation, TNF- $\alpha$  was used as a stimulator *in vitro* to induce inflammation in Beas-2B cells. As shown in Fig. 5, incubation with TNF- $\alpha$  markedly induced the expression of IL-1 $\beta$ , IL-6, MCP-1 and ICAM-1, while pretreatment with 2.5 or 5  $\mu$ M PL inhibited this increase in expression.

NF- $\kappa$ B is a transcription factor regulating the expression of genes participating in both the innate and adaptive immune response (35,36). NF- $\kappa$ B can regulate the expression of a number of inflammatory cytokines. In quiescent cells, NF- $\kappa$ B, an isomeric dimer consisting of the P65 and the P50 subunits, is located in the cytoplasm and is bound to an inhibitory protein, I $\kappa$ B, in an inactive state (37). Upon cell

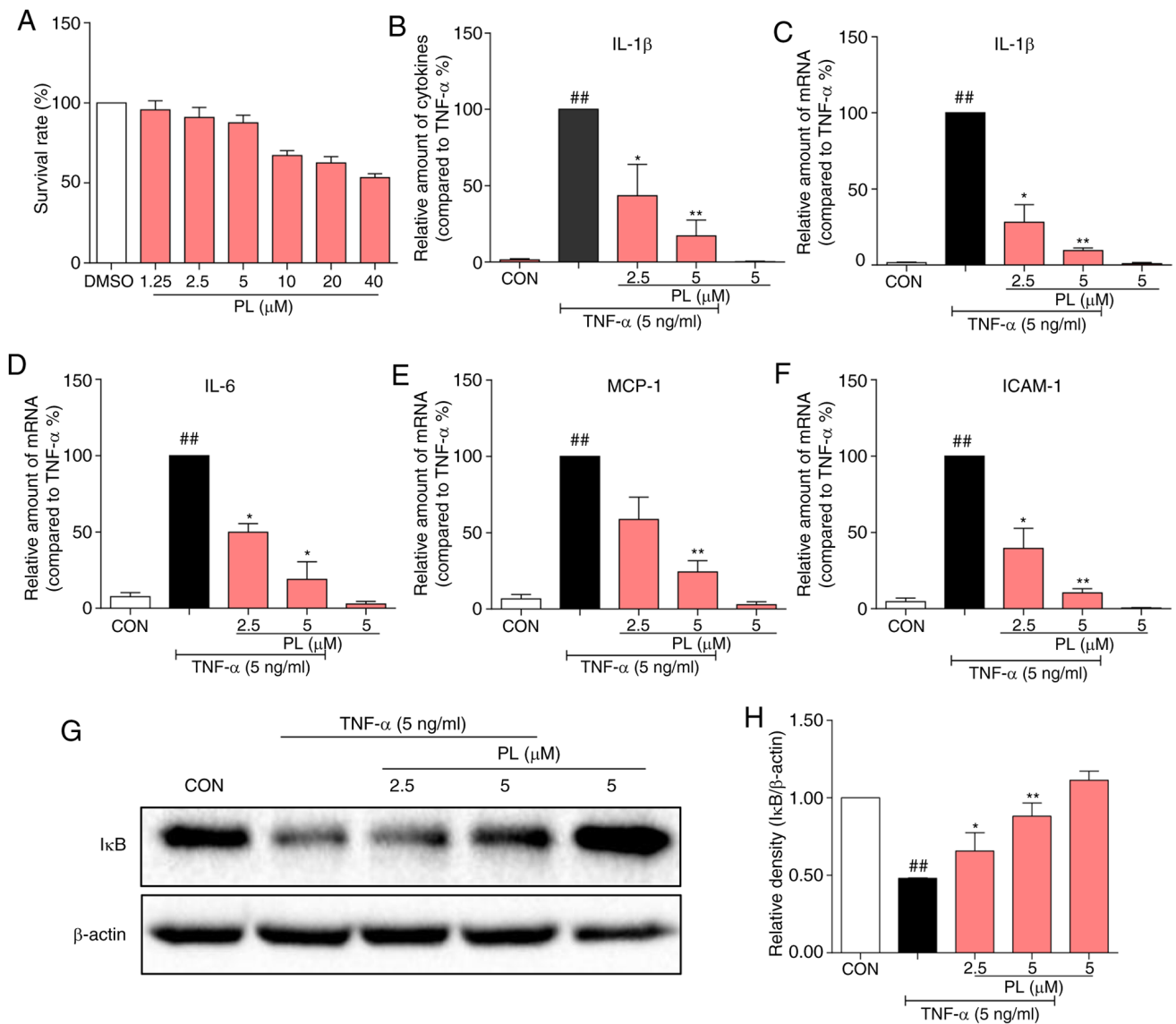


Figure 5. PL relieves TNF- $\alpha$ -induced inflammation by inhibiting NF- $\kappa$ B activation in Beas-2B cells. (A) Cytotoxic evaluation of PL (1.25, 2.5, 5, 10, 20 and 40  $\mu$ M) in Beas-2B cells. Beas-2B cells were pretreated with 2.5 or 5  $\mu$ M PL for 30 min and subsequently treated with or without 5 ng/ml TNF- $\alpha$ . (B) After TNF- $\alpha$  treatment for 24 h, the IL-1 $\beta$  levels in the medium were detected using ELISA. (C-F) After TNF- $\alpha$  treatment for 6 h, mRNA was collected. The gene expression of (C) IL-1 $\beta$ , (D) IL-6, (E) MCP-1 and (F) ICAM-1 were determined by RT-qPCR analysis using  $\beta$ -actin mRNA as the internal control. (G) After TNF- $\alpha$  treatment for 30 min, total protein was collected. The protein levels of I $\kappa$ B and  $\beta$ -actin were detected by western blotting. (H) Quantification for the density ratio of I $\kappa$ B and  $\beta$ -actin. Data are presented as the mean  $\pm$  standard error of the mean.  $^{##}P < 0.01$  vs. CON group;  $^{*}P < 0.05$ ,  $^{**}P < 0.01$  vs. TNF- $\alpha$  group. PL, piperlongumine; TNF, tumor necrosis factor; NF- $\kappa$ B, nuclear factor- $\kappa$ B; IL, interleukin; MCP, monocyte chemoattractant protein; ICAM, intracellular adhesion molecule; RT-qPCR, reverse transcription-quantitative polymerase chain reaction.

activation, I $\kappa$ B is degraded through a series of transduced signals to promote the translocation of P65 from the cytoplasm to the nucleus (37). Caramori *et al* reported that nuclear P65 expression was upregulated and cytoplasmic P65 expression was downregulated in the lung parenchyma and small airway epithelium in autopsy specimens from asthma patients compared with normal control subjects (38). Several stimuli that increase inflammation in asthma can activate NF- $\kappa$ B, including pro-inflammatory cytokines, allergens, ozone and viral infections (39). NF- $\kappa$ B activation in the asthmatic airway leads to increased expression of pro-inflammatory cytokines, inducible nitric oxide synthase and adhesion molecules, and may result in the amplification of the inflammatory response (39). Glucocorticoids, which are effective treatment agents for asthma, directly inhibit the activation of

NF- $\kappa$ B through a protein-protein interaction between glucocorticoid receptors and NF- $\kappa$ B (40,41). Thus, NF- $\kappa$ B may act as an attractive therapeutic target for asthma. A number of natural products, such as curcumin (42), pinocembrin (43), shikonin (44), osthole (45) and andrographolide (46), were reported to mitigate asthma in mice by modulating the activation of NF- $\kappa$ B. In the present study, I $\kappa$ B protein was found to be downregulated to undetectable levels in the lung tissues of asthmatic mice compared with control mice, whereas PL treatment reversed the decrease in I $\kappa$ B expression in a dose-dependent manner. These results indicate that PL exerts its anti-inflammatory effects in asthmatic mice by regulating the activation of NF- $\kappa$ B.

PL, a natural product isolated from the root of the long pepper *Piper longum* L, has been shown to effectively treat

asthma and chronic bronchitis (14). However, although several medicinal properties of PL have already been investigated, the exact anti-asthmatic effect of PL and the underlying mechanism have yet to be fully elucidated. In the present study, asthmatic mice administered PL exhibited less severe airway inflammation and remodeling compared with untreated asthmatic mice. PL has been reported to exert its anti-inflammatory effects by regulating the activation of NF- $\kappa$ B pathway in different inflammatory diseases. The results of the present study further confirmed that PL can reduce inflammatory response by inhibiting the activation of NF- $\kappa$ B.

In conclusion, the activity of PL against OVA-induced asthma and airway inflammation and the potential mechanisms were investigated in the present study. PL administration was found to reduce OVA-induced inflammatory cell infiltration, downregulate Th2 cytokine expression, and mitigate mucus secretion and airway fibrosis in asthmatic mice. The anti-inflammatory activity of PL may be attributed to its inhibitory effect on the activation of NF- $\kappa$ B. In TNF- $\alpha$ -stimulated Beas-2B cells, pretreatment with PL also downregulated the TNF- $\alpha$ -induced inflammatory cytokine expression and mitigated NF- $\kappa$ B activation. These results suggest that PL may be a promising candidate for the treatment of asthma by regulating NF- $\kappa$ B. However, further studies are required to fully elucidate the precise mechanism of NF- $\kappa$ B regulation by PL at the molecular level, and to verify the preclinical pharmacodynamics of PL in asthma.

#### Acknowledgements

Not applicable.

#### Funding

The present study was supported by the Natural Science Funding of China (grant nos. 81570027 to YD and 81872918 to YZ), the Zhejiang Provincial Natural Science Funding (grant nos. LY19H310001 to BZ, LY16H010007 to YD and LY17H010006 to LW).

#### Availability of data and materials

The datasets used and/or analyzed during the present study are available from the corresponding author on reasonable request.

#### Authors' contributions

YD and YZ designed the research study; CL, TX, WZ, BB, and ZX performed the research; CL, BZ, and YZ analyzed the data; BZ, LW and GL contributed essential reagents or tools; YD and YZ wrote the manuscript.

#### Ethics approval and consent to participate

This study was approved by the Committee on Animal Care of Wenzhou Medical University, Wenzhou, China.

#### Patient consent for publication

Not applicable.

#### Competing interests

The authors declare that they have no competing interests.

#### References

1. Network GA: The global asthma report 2018. <http://www.global-asthma-report.org/>
2. Papi A, Brightling C, Pedersen SE and Reddel HK: Asthma. *Lancet* 391: 783-800, 2018.
3. Robinson DS, Hamid Q, Ying S, Tsicopoulos A, Barkans J, Bentley AM, Corrigan C, Durham SR and Kay AB: Predominant Th2-like bronchoalveolar T-lymphocyte population in atopic asthma. *N Engl J Med* 326: 298-304, 1992.
4. Kidd P: Th1/Th2 balance: The hypothesis, its limitations, and implications for health and disease. *Altern Med Rev* 8: 223-246, 2003.
5. Olin JT and Wechsler ME: Asthma: Pathogenesis and novel drugs for treatment. *BMJ* 349: g5517, 2014.
6. Gray LE and Sly PD: Update in asthma 2017. *Am J Respir Crit Care Med* 197: 1108-1115, 2018.
7. Barnig C, Frossard N and Levy BD: Towards targeting resolution pathways of airway inflammation in asthma. *Pharmacol Ther* 186: 98-113, 2018.
8. Global Initiative for Asthma: GINA Report, Global strategy for asthma management and prevention (2015 update). <https://ginasthma.org/gina-reports/>
9. Dahl R: Systemic side effects of inhaled corticosteroids in patients with asthma. *Respir Med* 100: 1307-1317, 2006.
10. Roland NJ, Bhalla RK and Earis J: The local side effects of inhaled corticosteroids: Current understanding and review of the literature. *Chest* 126: 213-219, 2004.
11. Busse WW, Katial R, Gossage D, Sari S, Wang B, Kolbeck R, Coyle AJ, Koike M, Spitalny GL, Kiener PA, *et al*: Safety profile, pharmacokinetics, and biologic activity of MEDI-563, an anti-IL-5 receptor alpha antibody, in a phase I study of subjects with mild asthma. *J Allergy Clin Immunol* 125: 1237-1244.e2, 2010.
12. Leckie MJ, ten Brinke A, Khan J, Diamant Z, O'connor BJ, Walls CM, Mathur AK, Cowley HC, Chung KF, Djukanovic R, *et al*: Effects of an interleukin-5 blocking monoclonal antibody on eosinophils, airway hyper-responsiveness, and the late asthmatic response. *Lancet* 356: 2144-2148, 2000.
13. Flood-Page PT, Menzies-Gow AN, Kay AB and Robinson DS: Eosinophil's role remains uncertain as anti-interleukin-5 only partially depletes numbers in asthmatic airway. *Am J Respir Crit Care Med* 167: 199-204, 2003.
14. Bezerra DP, Pessoa C, de Moraes MO, Saker-Neto N, Silveira ER and Costa-Lotufo LV: Overview of the therapeutic potential of piperlongumine (piperlongumine). *Eur J Pharm Sci* 48: 453-463, 2013.
15. Zou P, Xia Y, Ji J, Chen W, Zhang J, Chen X, Rajamanickam V, Chen G, Wang Z, Chen L, *et al*: Piperlongumine as a direct TrxR1 inhibitor with suppressive activity against gastric cancer. *Cancer Lett* 375: 114-126, 2016.
16. Han JG, Gupta SC, Prasad S and Aggarwal BB: Piperlongumine chemosensitizes tumor cells through interaction with cysteine 179 of I $\kappa$ B $\alpha$  kinase, leading to suppression of NF- $\kappa$ B-regulated gene products. *Mol Cancer Ther* 13: 2422-2435, 2014.
17. Kim N, Do J, Bae JS, Jin HK, Kim JH, Inn KS, Oh MS and Lee JK: Piperlongumine inhibits neuroinflammation via regulating NF- $\kappa$ B signaling pathways in lipopolysaccharide-stimulated BV2 microglia cells. *J Pharmacol Sci* 137: 195-201, 2018.
18. Lee W, Yoo H, Kim JA, Lee S, Jee JG, Lee MY, Lee YM and Bae JS: Barrier protective effects of piperlongumine in LPS-induced inflammation in vitro and in vivo. *Food Chem Toxicol* 58: 149-157, 2013.
19. Sun J, Xu P, Du X, Zhang Q and Zhu Y: Piperlongumine attenuates collagen-induced arthritis via expansion of myeloid-derived suppressor cells and inhibition of the activation of fibroblast-like synoviocytes. *Mol Med Rep* 11: 2689-2694, 2015.
20. Zaynagetdinov R, Ryzhov S, Goldstein AE, Yin H, Novitskiy SV, Goleniewska K, Polosukhin VV, Newcomb DC, Mitchell D, Morschl E, *et al*: Attenuation of chronic pulmonary inflammation in A2B adenosine receptor knockout mice. *Am J Respir Cell Mol Biol* 42: 564-571, 2010.
21. Kim ST, Chun JW, Park G and Koh JW: Comparative quantification of plasma TDRD7 mRNA in cataract patients by real-time polymerase chain reaction. *Korean J Ophthalmol* 28: 343-350, 2014.

22. Ray A and Cohn L: Altering the Th1/Th2 balance as a therapeutic strategy in asthmatic diseases. *Curr Opin Investig Drugs* 1: 442-448, 2000.
23. Ray A and Cohn L: Th2 cells and GATA-3 in asthma: New insights into the regulation of airway inflammation. *J Clin Invest* 104: 985-993, 1999.
24. Truyen E, Coteur L, Dilissen E, Overbergh L, Dupont LJ, Ceuppens JL and Bullens DM: Evaluation of airway inflammation by quantitative Th1/Th2 cytokine mRNA measurement in sputum of asthma patients. *Thorax* 61: 202-208, 2006.
25. Steinke JW and Borish L: Th2 cytokines and asthma. Interleukin-4: Its role in the pathogenesis of asthma, and targeting it for asthma treatment with interleukin-4 receptor antagonists. *Respir Res* 2: 66-70, 2001.
26. Foster PS, Hogan SP, Ramsay AJ, Matthaei KI and Young IG: Interleukin 5 deficiency abolishes eosinophilia, airways hyper-reactivity, and lung damage in a mouse asthma model. *J Exp Med* 183: 195-201, 1996.
27. Wills-Karp M, Luyimbazi J, Xu X, Schofield B, Neben TY, Karp CL and Donaldson DD: Interleukin-13: Central mediator of allergic asthma. *Science* 282: 2258-2261, 1998.
28. Halwani R, Al-Muhsen S and Hamid Q: Airway remodeling in asthma. *Curr Opin Pharmacol* 10: 236-245, 2010.
29. Yao X, Wang W, Li Y, Lv Z, Guo R, Corrigan CJ, Ding G, Huang K, Sun Y and Ying S: Characteristics of IL-25 and allergen-induced airway fibrosis in a murine model of asthma. *Respirology* 20: 730-738, 2015.
30. An G, Zhang X, Wang W, Huang Q, Li Y, Shan S, Corrigan CJ, Wang W and Ying S: The effects of interleukin-33 on airways collagen deposition and matrix metalloproteinase expression in a murine surrogate of asthma. *Immunology* 2018 (Epub ahead of print).
31. Broide DH, Lotz M, Cuomo AJ, Coburn DA, Federman EC and Wasserman SI: Cytokines in symptomatic asthma airways. *J Allergy Clin Immunol* 89: 958-967, 1992.
32. Berry MA, Hargadon B, Shelley M, Parker D, Shaw DE, Green RH, Bradding P, Brightling CE, Wardlaw AJ and Pavord ID: Evidence of a role of tumor necrosis factor alpha in refractory asthma. *N Engl J Med* 354: 697-708, 2006.
33. Brown SD, Brown LA, Stephenson S, Dodds JC, Douglas SL, Qu H and Fitzpatrick AM: Characterization of a high TNF- $\alpha$  phenotype in children with moderate-to-severe asthma. *J Allergy Clin Immunol* 135: 1651-1654, 2015.
34. Thomas PS, Yates DH and Barnes PJ: Tumor necrosis factor-alpha increases airway responsiveness and sputum neutrophilia in normal human subjects. *Am J Respir Crit Care Med* 152: 76-80, 1995.
35. Baeuerle PA and Baichwal VR: NF-kappa B as a frequent target for immunosuppressive and anti-inflammatory molecules. *Adv Immunol* 65: 111-137, 1997.
36. Xiao C and Ghosh S: NF-kappaB, an evolutionarily conserved mediator of immune and inflammatory responses. *Adv Exp Med Biol* 560: 41-45, 2005.
37. Tak PP and Firestein GS: NF-kappaB: A key role in inflammatory diseases. *J Clin Invest* 107: 7-11, 2001.
38. Caramori G, Oates T, Nicholson AG, Casolari P, Ito K, Barnes PJ, Papi A, Adcock IM and Chung KF: Activation of NF-kappaB transcription factor in asthma death. *Histopathology* 54: 507-509, 2009.
39. Barnes PJ and Adcock IM: NF-kappa B: A pivotal role in asthma and a new target for therapy. *Trends Pharmacol Sci* 18: 46-50, 1997.
40. Adcock IM, Brown CR, Gelder CM, Shirasaki H, Peters MJ and Barnes PJ: Effects of glucocorticoids on transcription factor activation in human peripheral blood mononuclear cells. *Am J Physiol* 268: C331-C338, 1995.
41. Ray A and Prefontaine KE: Physical association and functional antagonism between the p65 subunit of transcription factor NF-kappa B and the glucocorticoid receptor. *Proc Natl Acad Sci USA* 91: 752-756, 1994.
42. Chauhan PS, Singh DK, Dash D and Singh R: Intranasal curcumin regulates chronic asthma in mice by modulating NF- $\kappa$ B activation and MAPK signaling. *Phytomedicine* 51: 29-38, 2018.
43. Gu X, Zhang Q, Du Q, Shen H and Zhu Z: Pinocembrin attenuates allergic airway inflammation via inhibition of NF- $\kappa$ B pathway in mice. *Int Immunopharmacol* 53: 90-95, 2017.
44. Wang TY, Zhou QL, Li M and Shang YX: Shikonin alleviates allergic airway remodeling by inhibiting the ERK-NF- $\kappa$ B signaling pathway. *Int Immunopharmacol* 48: 169-179, 2017.
45. Wang J, Fu Y, Wei Z, He X, Shi M, Kou J, Zhou E, Liu W, Yang Z and Guo C: Anti-asthmatic activity of osthole in an ovalbumin-induced asthma murine model. *Respir Physiol Neurobiol* 239: 64-69, 2017.
46. Li J, Luo L, Wang X, Liao B and Li G: Inhibition of NF-kappaB expression and allergen-induced airway inflammation in a mouse allergic asthma model by andrographolide. *Cell Mol Immunol* 6: 381-385, 2009.



This work is licensed under a Creative Commons Attribution-NonCommercial-NoDerivatives 4.0 International (CC BY-NC-ND 4.0) License.